

Holographic data storage with arbitrarily misaligned data pages

Geoffrey W. Burr

IBM Almaden Research Center, 650 Harry Road, San Jose, California 95120

Received October 24, 2001

An improved postprocessing algorithm that can compensate for arbitrary misregistrations between a detector array and the coherent image of a pixelated two-dimensional data page is described. Previously [Opt. Lett. **26**, 542 (2001)], an algorithm was reported in which both linear and quadratic interpixel cross-talk contributions are reallocated to the appropriate neighboring pixels. However, page misalignments close to ± 0.5 pixels could not be corrected to an acceptable bit-error rate because of propagation in the iterative procedure. An improved algorithm is reported in which an intentional magnification error is introduced optically and then corrected during postprocessing. Experimental results from a pixel-matched megapixel volume holographic system are presented, showing that the dependence of bit-error rate on transverse detector alignment is entirely removed. This improved procedure can completely bypass constraints on page registration, optical distortion, and material shrinkage that currently hamper page-oriented holographic storage systems. © 2002 Optical Society of America

OCIS codes: 210.0120, 100.0100.

Volume holographic data storage, in which data are modulated onto, stored as, and then retrieved from spatial optical wave fronts, has remained a compelling technology for many researchers despite numerous obstacles.¹ This technology offers the potential for both high capacity and high speed. The high capacity comes from storing as much as one bit for each cubic wavelength of storage medium; the high speed, from retrieving millions of these bits in parallel. Both of these features are made possible by the large pixelated data pages used for input and output.

One of the obstacles encountered by researchers has been the need for tight tolerances on the alignment, magnification, and imaging aberrations of these data pages to retrieve encoded data successfully.¹ In turn, the need to maintain these tolerances has dominated the engineering of all aspects of a holographic storage system that involve distortion or deflection of the retrieved data pages. These aspects include holographic readout from a spinning and wobbling disk,¹ thermal expansion,² changes in readout wavelength,³ and material shrinkage.⁴

One approach to bypassing these tight tolerances would be to postprocess each retrieved data page to extract the encoded data. Misalignments by an integer number of pixels are simple to correct, requiring only bookkeeping in reassigning pixels and redundant encoding of data at opposite edges of the page. Thus, it is necessary only to find an algorithm that can compensate for a residual fractional shift of up to ± 0.5 pixels.

Recently, an algorithm for postprocessing retrieved data pages was described that allows one to compensate for a moderate pixel shift.⁵ Experimental results showed a significant improvement in the range of page misalignments for which the raw bit-error rate (BER) remained acceptable (below 10^{-3}). However, when all the contributing factors at any given spot on the data page (such as global misalignment, magnification error, and distortion) led to a total local shift of ~ 0.5 pixels, the algorithm of Ref. 5 could not adequately

compensate. This Letter describes a significantly improved algorithm that can produce postprocessed data pages with acceptable raw BER, for any page alignment.

The previously reported⁵ shift-compensation algorithm operates by iteratively processing each row and column of the data page on a pixel-by-pixel basis. At each pixel, the detected intensity signal, r_2 , is separated into three components based on the known local shift, σ_x or σ_y : the surviving portion of the intended signal, p_2 , the linear cross talk coming from one of the neighboring pixels, p_1 , and the additional cross talk contributed by coherent interference between p_1 and p_2 .⁵ If the row (or column) is processed in the appropriate direction, then the value of p_1 is known from the previous iteration of the algorithm, and the desired result p_2 is the only unknown.

When the point-spread function (PSF) is separable (e.g., diffraction from a square Fourier-transform aperture dominates coma and spherical aberration), the algorithm can be extended to two dimensions simply by processing each dimension separately. Nonseparable PSFs can be treated by processing rowwise and columnwise to cover each possible set of three neighboring pixels (one horizontal, one vertical, and the associated diagonal pixel). Evaluating additional neighbors would make the algorithm noncausal, forcing multiple passes across the page to refine the iterative estimates. The conditions for a separable PSF applied in the DEMON II holographic storage platform,⁶ and the algorithm described above could significantly improve the raw BER over a wide range of page misregistrations.⁵ Similar results were obtained with the extended version for nonseparable PSFs,⁵ and preliminary results showed promising results for correcting small magnification errors that were due to material shrinkage.⁷

However, when the local pixel shift at any portion of the data page approached ~ 0.5 pixels, the value of p_2 was being extrapolated from the relatively small portion remaining within the detected signal, r_2 .

Random noise affecting r_2 was thus amplified and then corrupted the determination of the next pixel, and so on across the row. Some improvement was made by weighted averaging of the estimates of pixel values made on both passes (e.g., for rows, the left-to-right and right-to-left passes), instead of keeping only one of these estimates. Even so, a global page misregistration of ~ 0.5 pixels in x or y or both in DEMON II led to similar local shifts over wide portions of the data page and unacceptably high raw BER.⁵

It was postulated in Ref. 5 that introducing an intentional magnification error might possibly reduce the error propagation, since the rapidly changing local offsets would pass quickly through $|\sigma| \sim 0.5$ in isolated patches. Then all possible local shifts would be represented across the data page under any global misregistration, and the poor performance of the algorithm under a half-pixel shift would be balanced by the presence of data that are locally registered.

We experimentally implemented such an intentional magnification error with the DEMON III platform.⁸ This platform was built to evaluate phase-conjugate readout by use of a buffer hologram,¹⁰ a concept designed to make possible large-capacity read-write holographic data storage. A 1024×1024 nematic reflective liquid-crystal spatial light modulator¹ (SLM) and a 1024×1024 CCD camera (Dalsa CA-D4-1024; fill factor, $>90\%$) were placed at orthogonal faces of a polarizing beam-splitter cube (Fig. 1). The modulated object beam was recorded with a collimated reference beam in transmission geometry in a 1-cm³ cube of strontium barium niobate. After retrieval with a carefully aligned counterpropagating beam, the phase-conjugate object beam returned back through the same optical system and onto the detector array with low aberration. Each hologram was fully erased before the next was recorded with the same pair of beams.

The 12.8- μm pitch of the reconstructed data page landing on the 12.0- μm pixel pitch of the detector array should provide a magnification error of exactly 16:15 ~ 1.0667 . However, imperfections in the pseudo-phase-conjugate readout imposed deterministic variations of up to ± 0.2 pixels, analogous to moderate optical distortion. But since 15 pixels on the SLM corresponded to 16 on the detector, simple alignment patterns such as patterns of sparsely spaced lines or coarse checkerboards could be designed for direct detection. Finer-resolution patterns, such as the portion of a 1×1 pixel checkerboard pattern shown in Fig. 2(a), showed the expected variation from local alignment to half-pixel misalignment and back again over every 16 pixels. Figure 2(b) shows the results of postprocessing the received data page in Fig. 2(a) with a modified version of the shift-compensation algorithm: The original 1×1 checkerboard pattern is successfully recovered.

Although the same binomial equation from Ref. 5 was iteratively solved to correct each pixel, changes were required in most other aspects of the algorithm. As in Ref. 5, the total local shift σ used at each iteration of the algorithm was the sum of a static local

shift (the distortion pattern, saved in a lookup table) and a dynamic global shift (the overall page misalignment, measured with fiducial marks). But here the local shifts representing the magnification error and distortion map were interpolated for each pixel from a precalibrated grid. Page translations were performed by movement of the Dalsa camera chip with an xy piezo-translation stage. Algorithm parameters (H_{00} , H_{01} , and H_{11} from Ref. 5) were similarly calibrated with single- and double-line patterns for $-1.0 < \sigma < 1.0$ to a resolution of 0.025 pixels.

In addition to the static local shift σ , it was also necessary to keep a map of integer pixel offsets between the raw data and the postprocessed output. For instance, note that the outermost rows and columns of Fig. 2(b) must originate from raw data pixels outside of the portion shown in Fig. 2(a), so that the number of SLM pixels and postprocessed data pixels match. At the boundaries of the detected data page, this integer offset between raw data and destination reached ± 32 pixels.

These regions with identical integer pixel offset then move with data-page translation, as the global misregistration of the data page is added to each static local offset to produce σ . Measuring the global misregistration with the isolated fiducial pixels used with DEMON II proved to be too inaccurate. These pixels were supplemented with four small blocks of 1×1 checkerboard patterns, either 8×20 or 20×8 pixels, surrounded by a 2-pixel ring of OFF pixels. The shift algorithm was then repeatedly performed only in these four small regions for estimation of the correct global x and y page shift.

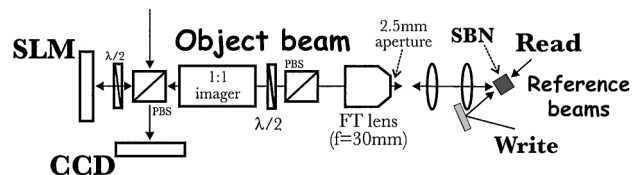


Fig. 1. Relevant portion of DEMON III holographic storage platform.⁸ Holograms are written in a strontium barium niobate (SBN) crystal, retrieved with a pseudo-phase-conjugate reference beam, and then erased. $\lambda/2$'s, half-wave plates; PBS, polarizing beam splitter; FT, Fourier-transform.

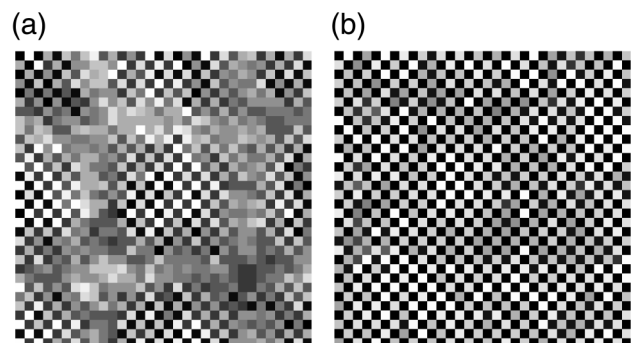


Fig. 2. Portion of a 1×1 checkerboard pattern (a) as relayed directly from the SLM plane (12.8- μm pitch) to the CCD plane (12.0- μm pitch) by phase-conjugate holographic reconstruction and (b) after correction with the improved shift-compensation algorithm.

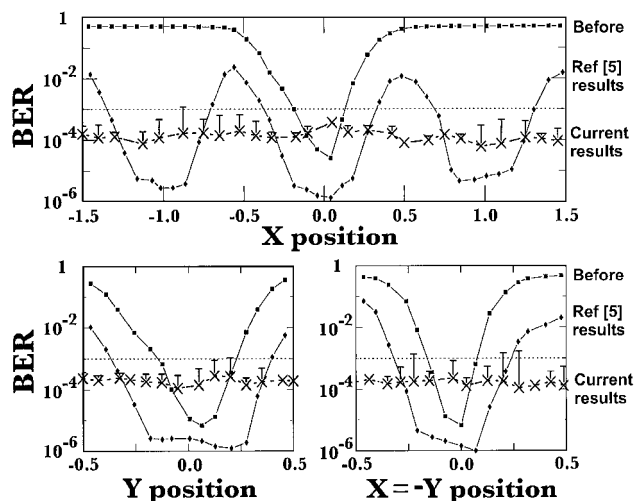


Fig. 3. Dependence of the raw BER (with an 8:12 modulation code¹⁰), before and after shift-compensation postprocessing, as a function of (a) x shift, (b) y shift, (c) shift along $x = -y$. The data from Ref. 5 were taken under 1:1 imaging on DEMON II⁶; the data for the improved shift-compensation algorithm were taken under 16:15 magnification by phase-conjugate readout on DEMON III.⁸

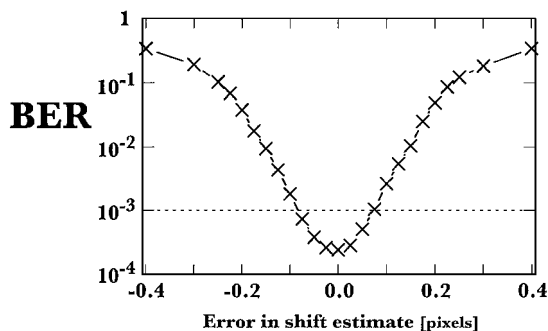


Fig. 4. Dependence of raw BER, averaged over ten pages, when shift-compensation postprocessing is performed with different estimates of the global x misregistration.

In the resulting postprocessed data pages, errors tended to congregate in the rows and columns where the total local shift passed through $|\sigma| \sim 0.5$. These concentrated regions of poor signal-to-noise ratio overwhelmed the soft error correction provided by the 8-bits-from-12-pixels modulation decoder that was used.¹⁰ However, locally interleaving these regions of high and low signal-to-noise ratio before demodulation produced a significantly lower raw BER.

In Fig. 3 the resulting pagewide ($\sim 900,000$ pixels) raw BER is plotted as a function of global x shift, y shift, and shift along the $x = -y$ diagonal. The modified shift algorithm with intentional magnification error is compared with the results of Ref. 5 and is shown to produce an average raw BER of 1.75×10^{-4} , independently of pixel shift. The \times 's in Fig. 3 represent the best-case BER resulting from the optimal choice of global x and y misregistration; each error bar shows the higher BER that resulted when the

global misregistration was estimated with just the four small fiducial blocks. This discrepancy implies that an even more accurate method of estimating the dynamic global misregistration in the presence of scatter and detector noise will likely be needed. Figure 4 quantifies the importance of using the correct global misregistration, showing average raw BER as the x global misregistration varies around the optimal value. However, holographic storage systems must already measure and then correct page misalignment to nearly this same accuracy (see the top set of curves in Fig. 3). Shift compensation requires slightly better measurement accuracy but removes the need to correct the alignment.

The 16:15 magnification error used here was dictated by the available components. An optimal choice of magnification error would have to balance the improvement in the shift-compensation algorithm and the space needed to measure page translation against the encoding efficiency (amount of data delivered per detector pixel).

In conclusion, intentionally introducing a magnification error makes it possible to retrieve coherent pixelated data under arbitrary misalignment. The need to minimize the misalignment and distortions of the data page is replaced by the need to know the exact misalignment and distortion pattern. Redundantly encoding data at the opposite edges of a SLM containing more pixels than the detector array should make it possible to design in tolerance for misregistrations of tens or even hundreds of pixels. This approach has the potential to open up numerous trade-offs in holographic data storage, including material shrinkage, thermal expansion, readout at different wavelengths, and readout from moving storage media.

G. Burr's e-mail address is burr@almaden.ibm.com.

References

1. H. J. Coufal, D. Psaltis, and G. Sincerbox, eds., *Holographic Data Storage* (Springer-Verlag, Berlin, 2000).
2. R. DeVre, J. F. Heanue, K. Gurkan, and L. Hesselink, *J. Opt. Soc. Am. A* **13**, 1331 (1996).
3. D. Psaltis, F. Mok, and H. S. Li, *Opt. Lett.* **19**, 210 (1994).
4. R. M. Shelby, D. A. Waldman, and R. T. Ingwall, *Opt. Lett.* **25**, 713 (2000).
5. G. W. Burr and T. Weiss, *Opt. Lett.* **26**, 542 (2001).
6. G. W. Burr, C. M. Jefferson, H. Coufal, M. Jurich, J. A. Hoffnagle, R. M. Macfarlane, and R. M. Shelby, *Opt. Lett.* **26**, 444 (2001).
7. G. W. Burr, T. Weiss, and R. M. Shelby, *SPIE Holography Newsletter* **11**, 4 (2000).
8. G. W. Burr, E. Mecher, T. Juchem, K. Meerholz, and N. Hampp are preparing a manuscript entitled "Multiplexed volume holographic storage using a phase-conjugate buffer hologram: demonstration and system considerations."
9. G. W. Burr and I. Leyva, *Opt. Lett.* **25**, 499 (2000).
10. G. W. Burr, J. Ashley, H. Coufal, R. K. Grygier, J. A. Hoffnagle, C. M. Jefferson, and B. Marcus, *Opt. Lett.* **22**, 639 (1997).